KAWASAKI STEEL TECHNICAL REPORT
No.3 (September 1981)

Reconstruction of Mizushima No.2 Blast Furnace for the Third Campaign

Keigo Kadomoto, Nobunao Kato, Toru Ishihara, Masasuke Oishi

Synopsis :
No.2 blast furnace at Mizushima Works was blown out on July 31, 1978 and blown in on March 20, 1979 for the third campaign. The period of a little over seven months is considered reasonable from economic viewpoint. With major reconstruction work including the blowing-out without burden, the slow cooling of hot stoves, and the following items all carried out within and by the company alone, the recent work indicates a sufficient capability of the company in this field covering hardware and software including manning to a point of practical application anywhere: (1) New approaches for prolongation of blast furnace compaign life, (2) A new way of taking in shell plates and large bell from the furnace bottom, (3) Automatic horizontal welding machine for girth seams on shell plates, (4) A new retractable hood for secondary dust collection around the tap hole, and (5) Molten slag cooler (called K-N type) for high-density granulated slag.

The body can be viewed from the next page.

Reconstruction of Mizushima No. 2 Blast Furnace for the Third Campaign*

Keigo KADOMOTO** Nobunao KATO** Toru ISHIHARA**
Masasuke OISHI**

No. 2 blast furnace at Mizushima Works was blown out on July 31, 1978 and blown in on March 20, 1979 for the third campaign. The period of a little over seven months is considered reasonable from economic viewpoint. With major reconstruction work including the blowing-out without burden, the slow cooling of hot stoves, and the following items all carried out within and by the company alone, the recent work indicates a sufficient capability of the company in this field covering hardware and software including manning to a point of practical application anywhere:

(1) New approaches for prolongation of blast furnace campaign life,
(2) A new way of taking in shell plates and large bell from the furnace bottom,
(3) Automatic horizontal welding machine for girth seams on shell plates,
(4) A new retractable hood for secondary dust collection around the tap hole, and
(5) Molten slag cooler (called K-N type) for high-density granulated slag.

1 Introduction

No. 2 blast furnace at Mizushima Works was blown out on July 31, 1978 and blown in again on March 20, 1979 as planned.

This reconstruction project was the first such project ever to be planned and executed entirely within the company, with its careful consideration of not only minimizing reconstruction costs but also of determining investment from a new concept of the minimum life cycle cost of equipment. As a result, the project was completed with only 65% of what it conventionally required.

Throughout the reconstruction of this blast furnace examinations were carried out and innovations added, with emphasis placed upon the following points:

(1) Development of new technology (empty blowing-out and slower hot stove cooling)
(2) Extended blast furnace life
(3) Reductions in reconstruction and operating costs, and reduced energy consumption
(4) Improved dust collecting methods for cast house

The purpose of this report is to explain the feature of technology used for the reconstruction of No. 2 blast furnace, and to outline the facilities.

Photo. 1 shows an entire view of a new No. 2 blast furnace, and **Table 1** lists the items of reconstruction and major specifications of the furnace.

2 Blowing-out

2.1 Empty Blowing-out Method

For this blast furnace the empty blowing-out operation method was adopted. In implementing this method, a rapid increase in temperature at the furnace top due to channeling, and the resulting equipmental damage and trouble by in-furnace gas explosion were anticipated. For this reason the following special measures were taken:

(1) Blast volume was calculated considering in-furnace gas velocity at the limit of channeling. Also considered was difference in gas velocity at the center and at the walls of the furnace.
(2) Existence of channeling was checked by the analysis of the top gas. Here the control value was set at a 0.2% oxygen concentration, with measures such as lowering of wind volume taken when oxygen content exceeds it.
(3) A video camera was used for constant observation of the tuyere so that remedial action i.e. wind

* Originally published in *Kawasaki Steel Technical Report*, **12** (1980) 2, pp. 23–34 (in Japanese)
** Mizushima Works

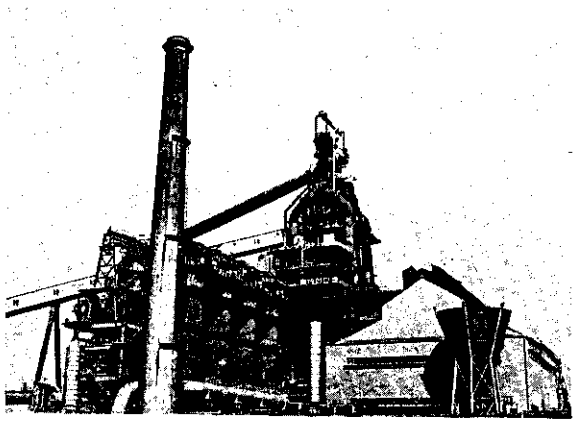

Photo. 1 No. 2 blast furnace at Mizushima Works

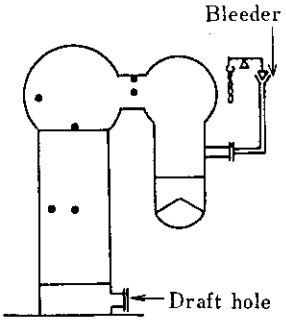

• means a position of thermocouple

Fig. 1 Slow cooling arrangement of hot stove

reduction, etc. can be taken immediately at the time of emergency.

With the empty blowing-out process progressed almost as planned, the subject operating technique has been established.

2.2 Slower Hot Stove Cooling

At the time of reconstructing No. 2 blast furnace for the second campaign, major parts of the hot stoves, including the shell plates and bricks, were replaced, and some modern innovations at that time were made. Careful operational control since then, kept the unit operating in nearly perfect condition. The checker work did not show any abnormal change in pressure loss due to aging. For these reasons, it was determined that the same hot stoves would be used again for the third campaign.

For the holding of the hot stoves during the reconstruction period, the slow cooling was taken followed by the holding at room temperature because of its cost advantage, despite its method for further study, over the holding method at a higher temperature range.

In slow-cooling the hot stoves, special attention was given to the silica bricks which, because of their peculiar zone for rapid heat expansion changes, could be cracked if cooled improperly. The slow cooling method was determined only after a thorough technical study using calculation of heat transfer. The final decision called for natural cooling, in particular, with the air completely shut-off and natural ventilation employed to speed up the process when the work got behind schedule. **Fig. 1** shows the arrangement of the hot stove during slow cooling.

Fig. 2 shows how the actual cooling process went. The cooling rate was faster than originally planned, but the bricks still remained in good enough condition after the cooling process was finished, determined to be reusable with no problem.

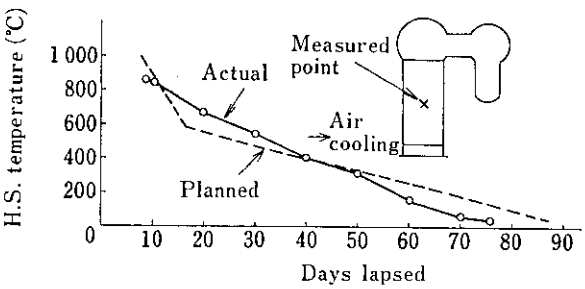

Fig. 2 Cooling performance of No. 5 hot stove

Ever since operations began in the second campaign, pressure losses of checker chamber have been measured regularly to determine the friction factor k using the formula below. In this way it is possible to determine changes and deformation, if any, of checker bricks; information which helps to develop improved methods for operation and maintenance of hot stoves. As shown in **Table 2** and **Fig. 3,** there is fortunately no great change in friction factors as a result of hot stove cooling.

$$k = \Delta P_g/(\rho v^2/2g) \quad \cdots\cdots (1)$$

ΔP_g: Pressure loss through checker bricks (kgf/m²)
ρ: Waste gas density (kg/m³)
v: Waste gas velocity (m/s)
g: Acceleration of gravity (m/s²)

The hot stove has operated smoothly ever since the blowing-in of the third campaign, which confirms the fact that the subject slow cooling of hot stoves serves for the repeated use of bricks.

Table 1 General and reconstruction items of Mizushima No. 2 blast furnace and auxiliary equipments

Main specifications		Reconstructed items
Blast furnace		
Type	Free standing	Renewed: Furnace shell;Brickworks;Staves; Piping for water cooling of furnace body
Daily production	6 000 t/d	
Inner volume	2 857 m^3	
Hearth diameter	11.8 m	
Tapholes	3	Repaired: Shaft decks;Water circulation pumps for staves;Chemical dosing equipments and heat exchanger of stave cooling water
Cinder notches	0	
Tuyeres	33	
Cooling system		
Bottom	Water conduit	
Shaft, belly, bosh	Stave cooling	
Hearth	Water spray	
Hot stove		
Type	Koppers type with external combustion chamber	Newly installed: Air preheater
Number of stoves	4	Renewed: Ceramic burner;Refractories for hot blast branch pipes;Expansion joints of hot blast main pipe
Heating area per a stove	51 800 m^2	
Max. dome temperature	1 450℃	Repaired: Hot stove valves
Blast temperature	1 350℃	
Blast pressure	4.7 kgf/cm^2	
Blast volume	6 300 Nm^3/min	
Burner capacity per a stove	80 000 Nm^3/h	
Fuels	Mixture of B.F.and coke oven gases	
Air preheater	IHI Rothemuehle type	
Charging equipment		
Type	2-bell, 1-valve seal type	Renewed: Large bell;Lower parts of large bell cup and small bell;Movable armor plates
Diameter of large bell	6.8 m	
Diameter of small bell	2.96 m	Repaired: Valves for pressure equalizing and relieving;Gas seal valves;Dust collector;Oil unit for bells and revolving chute;Driving unit of movable armor;Stock line detector
Movable armor	GHH type	
Top gas pressure	Max. 2.5 kgf/cm^2	
Material feeding equipment		
Ore bins	16-400 m^3, 4-250 m^3	Renewed: Screen for sinter;Charging conveyer belt
Coke bins	4-850 m^3	
Weighing hoppers for ores	16-11 m^3, 4-4 m^3	Repaired: Coke bins;Feeders for ore and coke; Hopper scales;Driving units of belt conveyor;Charging belt conveyor gallery;Dust collector for stock house
Weighing hoppers for cokes	2-55 m^3	
Coke screens	2	
Aperture : Upper	60 mmϕ	
: Lower	33 mmϕ	
Ore screens	12	
Aperture : Upper	6×11×550 (l)mm	
: Lower	3×6×25 (l)mm	
Charging conveyer		
Width	2 000 mm	
Belt speed	120 m/min	
Capacity	3 400 t/h	

Cast house and auxiliaries		
Cast floors	Two floors on the opposite side of the furnace	Renewed: Splash covering crane;Tapping machine
Mud guns	3	Repaired: Cast houses;Cast floors;Mud guns and relating oil units
Type	All oil pressure	
Mud volume	0.25 m^3	
Openers	3	
Splash covering cranes	3	
Type	Wall crane	
Capacity	12 t	
Dust collector		
Type	Dry type(Bag filter)	
Capacity	20 000 Nm^3/min	
Outlet dust content	0.01 g/Nm^3	
Gas cleaning equipment		
System	Dust catcher Venturi scrubber Electric precipitor	Renewed: Throat assembly of venturi scrubber; Water feeding and drainage piping of venturi scrubber and electric precipitator
Capacity	510 000 Nm^3/h	
Outlet dust content	0.005 g/Nm^3	Repaired: Dust discharge equipment of dust catcher;Power pack of electric precipitator
Top gas pressure recovery turbine		
Type	Radial type	Repaired: Turbine;Generator (Turbine impeller was remodeled to increase output)
Output	8 200 kw	
Slag granulation equipment		
Capacity(t/min)	Nor. 3, max. 9, 5	All equipment was newly installed
Capacity of slag cooler for high density granulated slag(t/min)	Nor. 3, max. 5	

Table 2 Friction factors before and after cooling of hot stove

	#5HS	#6HS	#7HS	#8HS	Mean
Before cooling	71	87	72	75	76
After cooling	76	75	57	67	69

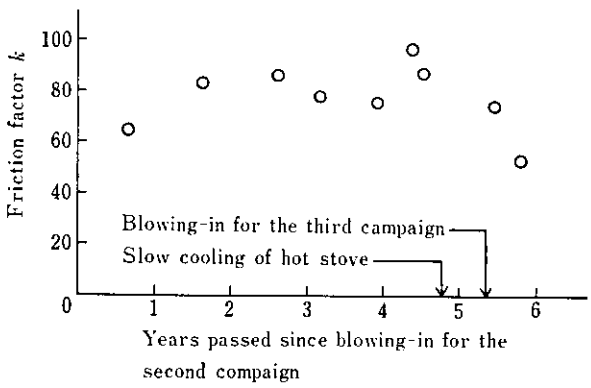

Fig. 3 Secular change of friction factor of No. 6 hot stove

3 Blast Furnace Shell Plates—Design and Construction

This was the first time that blast furnace shell plates were designed and manufactured within the company.

3.1 Design

For the furnace life, the designing of shell plates is as important as brick work and furnace body cooling facilities.

For design and construction of each part, it becomes necessary to calculate the forces (material force and internal stress) on each part of the blast furnace. This is calculated using an analytical system comprising a three dimensional skeleton structure, as showin in the skeleton structure model in **Fig. 4,** in which the four columns are connected to the dust catcher and the blast furnace body. Calculations are also made for such conditions as operation under high top pressure, shut-down of blast, operation during earthquakes, etc. These calculations were facilitated by the use of periphery-programs (Pre & post processor programs, the sectional coefficient of the calculation program, and the extremum detecting faculty which includes resultant internal stress) all of which were made by the company.

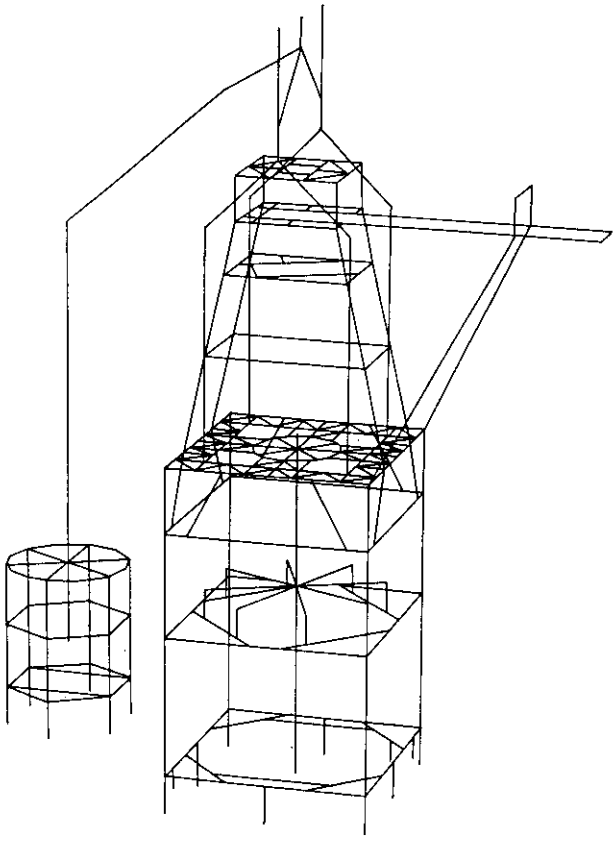

Fig. 4 Skelton structure model for coupled three dimensional structural analysis

Table 3 Grade of shell plate used for No. 2 blast furnace

	Steel grade	Thickness of shell plate(mm)
Bottom shell	JIS G3106 SM50B-N	60
Shell around tap hole		75
Shell around tuyeres		80
Bosh shell	JIS G3106 SM41-N	70
Belly shell		60
Shaft shell(1)		55
Shaft shell(2)		40

As for the furnace body, internal stress on each part was calculated based upon every working force in effect on the body. For these calculations, results from experiments performed separately within the company on photoelasticity experiments, analysis of internal stress around apertures by the finite element method, and analysis of internal stress on knuckle sections of the furnace body were employed.

These internal stress conditions were evaluated according to requirements under the ASME Code, Sec. III, in order to design the sound shell plates.

In order to ensure longer life, crack-resistant materials were employed and furnace shell was made in larger segments by using wide steel plates from the Mizushima No. 2 plate mill. **Table 3** shows the material and the thickness of the shell plates used at this time.

3.2 Manufacturing

In the manufacture of shell plates for this blast furnace, maximum use was made of advanced technology and various types of large-scale equipment which have been employed for years in the manufacture of welding structures for large vessels.

In manufacturing these shell plates, the following modifications were implemented on welding equipment in order to save man power and to improve quality and efficiency.

(1) Automatic horizontal welding machine[1] was developed, which consumed less man power than conventional manual horizontal welding methods.
(2) Welding of the 12 m cascade of shell plates including the 2 knuckles was made possible by

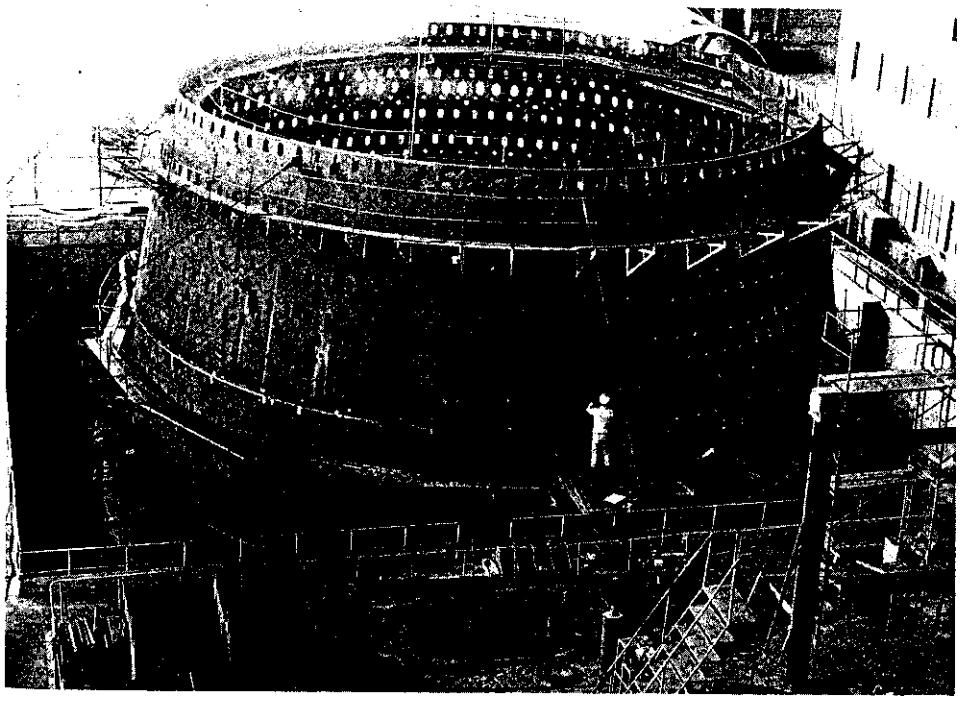

Photo. 2 Pre-assembled shell of No. 2 blast furnace

improvements in the consumable nozzle electroslag welding method. This also led to the successful enlarging of shell plate blocks.

Photo. 2 shows the pre-assembled shell of the blast furnace.

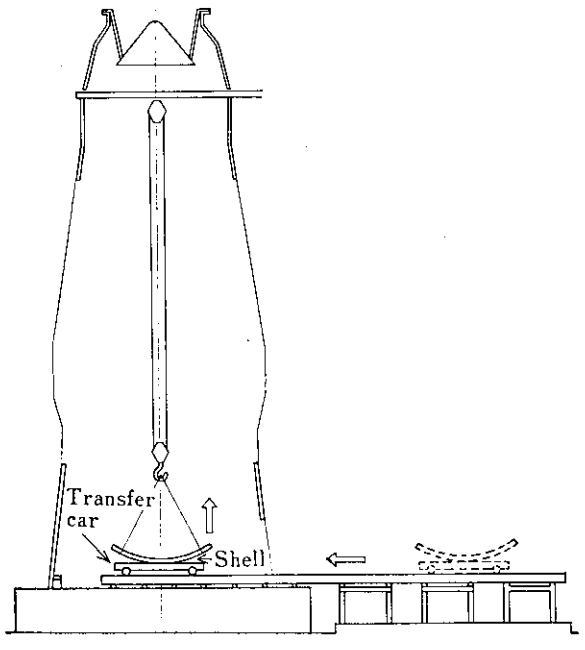

Fig. 5 New handling way of blast furnace shell plates and large bell

3.3 Construction

Conventional reconstruction methods called for disjointing the whole set of charging equipment at the furnace top and installing shell plates and large bell for the furnace through the upper portion of it with furnace-top cranes.

For this reconstruction, however, a sufficient equipment analysis was made prior to determining the scope of reconstruction with a life cycle cost concept taken into consideration, and reconstruction execution methods also carefully examined. The results were as shown in **Fig. 5**, in which the charging equipment at the furnace top was disjointed at the minimum, and a new method was adopted in which shell plates and the large bell were carried up through the furnace bottom instead of from outside. This new method greatly reduced reconstruction costs.

4 Cooling of the Furnace Body

4.1 Cooling of the Sidewall of the Bottom

In the second campaign the stave method was adopted for the cooling of the sidewall of the bottom in No. 2 blast furnace. This time, however, the heat transfer analysis was employed in order to compare the effectiveness of the stave cooling and the water spray cooling methods for brick work. The finite element method was employed in the heat transfer analysis, and the following three cases were analyzed:

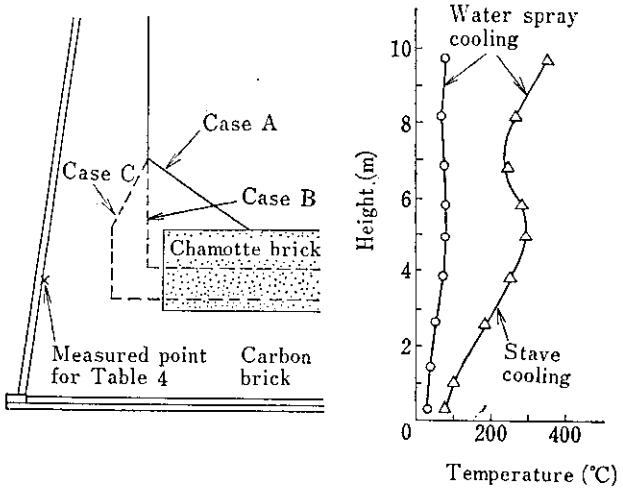

Fig. 6 An example of calculated temperature at brick surface of blast furnace bottom in the form of case C shown in the figure

Table 4 Calculated surface temperatures* of carbon bricks with different cooling methods for three cases of erosion

Case	Cooling method		Difference (1)-(2)
	(1)Stave	(2)Water spray	
A	100	42	58
B	181	55	126
C	291	76	215

* Temperature at × point in Fig.6

Case A: At the beginning of blast furnace operation

Case B: When the number of chamotte bricks is reduced to a half

Case C: When the remaining chamotte bricks are 200 mm thick

Cooling results are calculated by comparing temperatures at the same position. Results of these calculations are illustrated in **Fig. 6**. In addition, **Table 4** compares the surface temperatures of carbon bricks at point × in **Fig. 6**.

From these results, the water-spray cooling method which was considered more effective was used for the cooling of the bottom wall of No. 2 blast furnace in the third campaign. Also, Al was sprayed on the shell plates in order to prevent heat transfer loss due to scale formation on the bottom shells.

4.2 Shell Plate Protection Measures

Researches on blown-out blast furnaces revealed that positions of cracks that occurred in shell plates corresponded to the places where staves had disappeared, exposing the internal surfaces of shells. A network of cracks, such as those shown in **Photo. 3** was observed on the internal surface of the neighborhood of a shell-piercing crack. Research and experiments were performed in order to find the cause of these cracks.

Rapid shell temperature change was observed in the lower shaft as shown in **Fig. 7**, where it was supposed that the staves had fallen off. From this result, heat load during periods of rapid temperature change was calculated, and in turn, a schematic model of heat conditions was made, as shown in **Fig. 8**, while thermal stress distribution was calculated using the atypical elasticity finite element method. The results proved that compression stress higher than yield stress occurs in shell plates when heated, as shown in **Fig. 9**. It is considered that a plastic deformation as a result of compressive stress in heating leads to the generation of tensile stress when the shell temperature returns to normal, thereby causing the cracks.

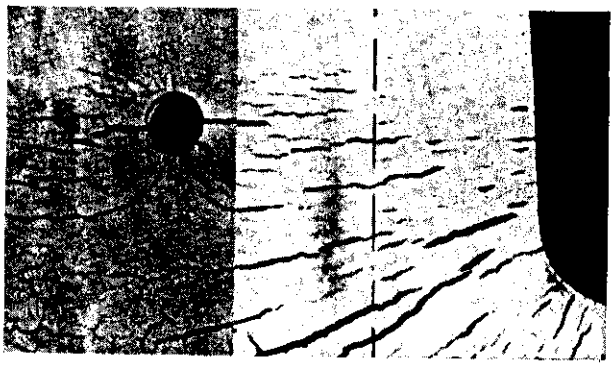

Photo. 3 Cracks in blast furnace shell plate

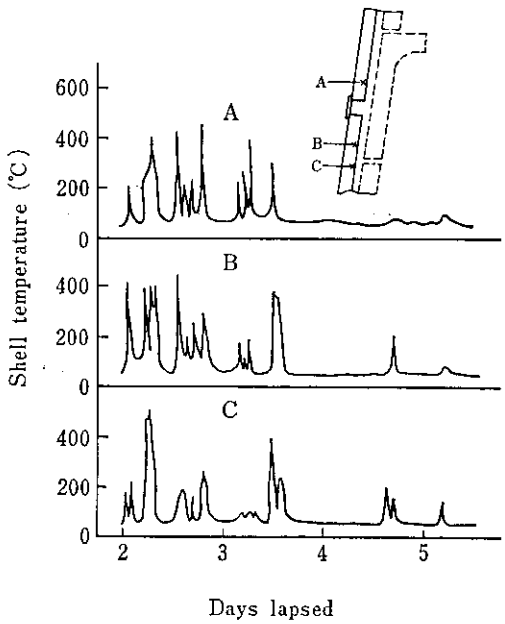

Fig. 7 Temperature change of blast furnace shell measured at 10 mm inside from the inner surface

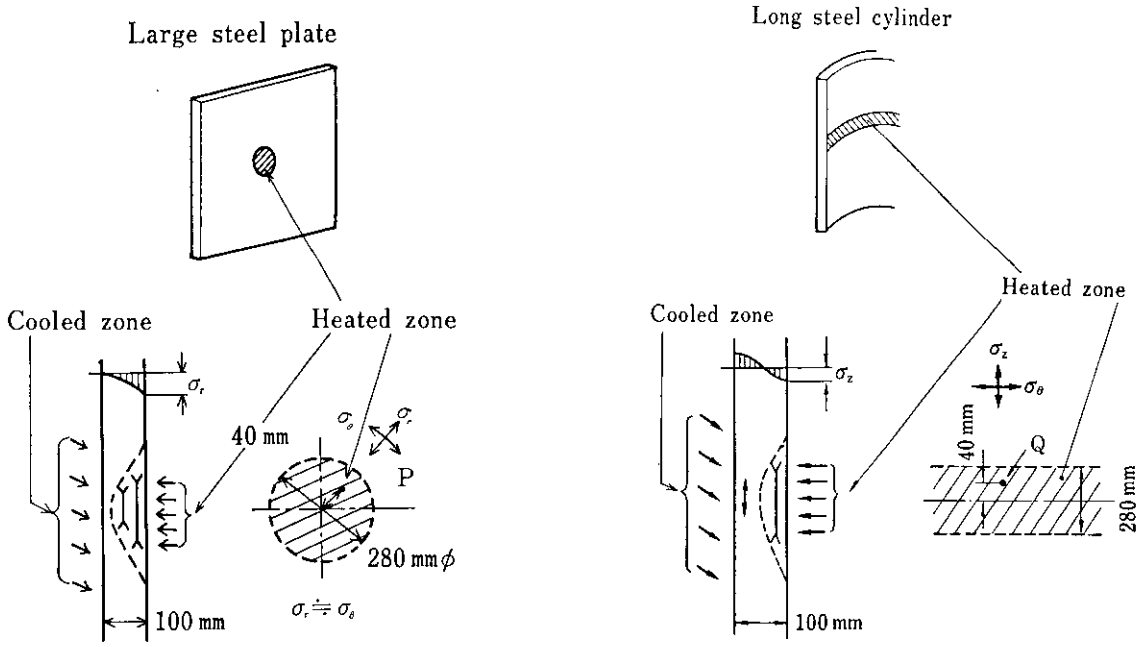

(a) Circular heating model (b) Ring-neck heating model

Fig. 8 Schematic modelling of heated shell for calculating thermal stress distribution

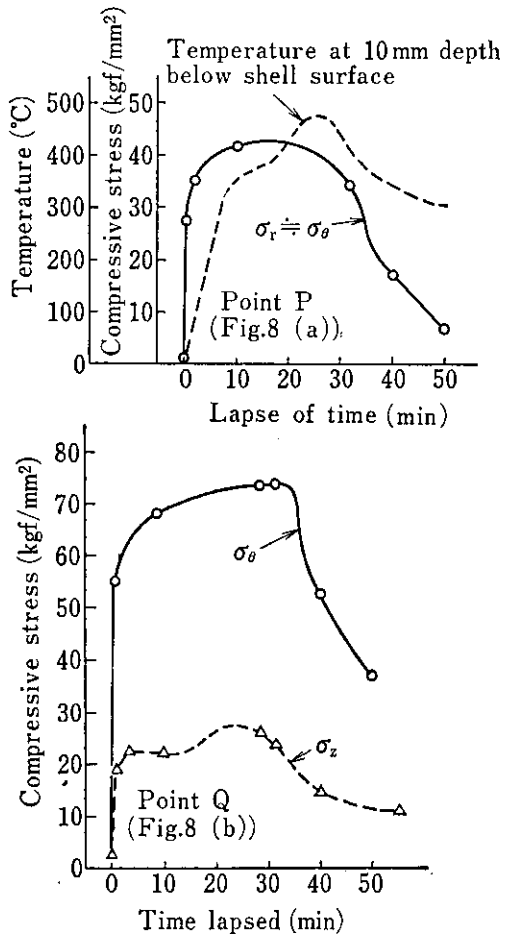

Fig. 9 Change of stress with time calculated at P and Q points shown in Fig. 8

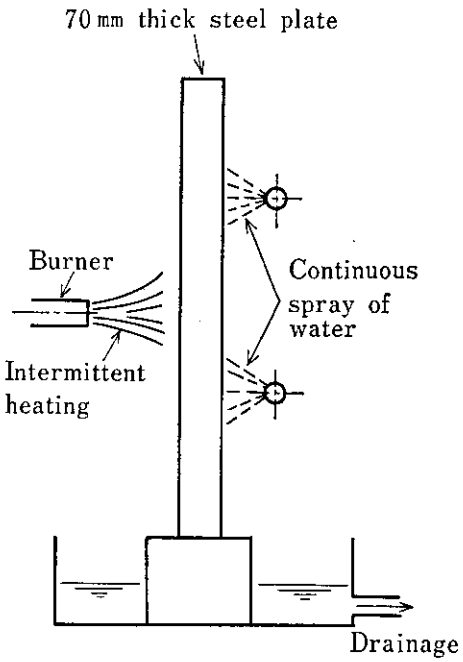

Fig. 10 Schema of crack test of steel plate

An experiment was carried out to reproduce cracks in the manner described in **Fig. 10,** and cracks were reproduced through repeated heating and cooling.

Through such research on shell plate cracks, it was thought necessary to contrive measures which would prevent the shells from being exposed to heated gas even after staves and bricks fell off.

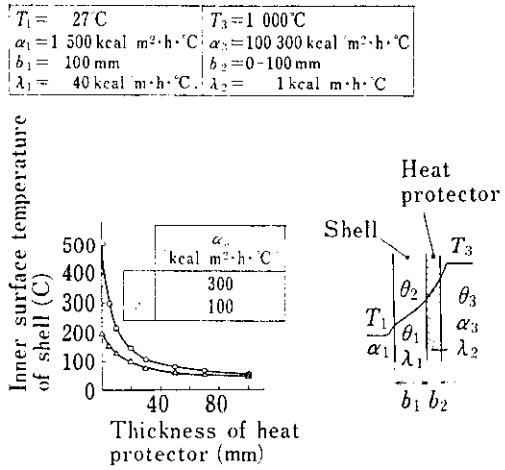

Fig. 11 Calculated effect of heat protector thickness of inner surface temperature of shell

A protective layer was thus placed on the internal surface of the shell plates in No. 2 blast furnace in order to protect them from heated gas. **Fig. 11** shows the method for calculating the anticipated temperature reduction in this case.

5 Examination of Brick Work and Estimation of Erosion

5.1 Bricks in the Belly—Lower Shaft Part of the Furnace

The belly—lower shaft part of the furnace as well as the bottom is the most important sector in determining the furnace life. In selecting bricks for these parts, therefore, reference was made to the result of in-company comparative tests on various bricks, with chemical erosion and thermal shock fracture also taken into consideration, so as to come up with a comprehensive judgement.

First of all, a resistance coefficient against thermal shock fracture was calculated using the following formula:

$$R = \frac{S(1-\mu)\cdot k}{E\cdot\alpha} \quad \cdots\cdots(2)$$

R: Resistance coefficient against thermal shock fracture (kcal/m·h)
S: Compression strength (kg/cm²)
μ: Poisson ratio
k: Thermal conductivity (kcal/m·h.°C)
E: Elasticity rate at normal temperature (kgf/cm²)
α: Linear expansion coefficient (°C⁻¹)

Secondly, for chemical erosion, the residual thickness of bricks under thermal equilibrium, S_X, was calculated according to the Koenig theory which states that erosion of bricks is controlled by chemical reaction rate, with the rate reduced by decreases in temperature, and that erosion of bricks ceases when the temperature falls below a certain point.

Table 5 Comparison of R* and S_X** for various bricks

Type of brick	R (kcal/m·h)	$10^3 S_x$ (m)
Chamotte brick (Al=43%, λ=1.3 kcal/m·h·℃)	3×10^2	7
High alumina brick (Al=97%, λ=9 kcal/m·h·℃)	17×10^2	140
SiC-C brick (SiC=78%, λ=15 kcal/m·h·℃)	47×10^2	653
Carbon brick (λ=12 kcal/m·h·℃)	42×10^2	312

* R: Coefficient of resistance against thermal shock fracture
** S_x: Residual thickness of brick under thermal equilibrium

Table 5 shows the R and S_X figures for various bricks. Bricks with larger figures for both R and S_X are prefered, with SiC-C bricks found to be the best.

In addition, SiC-C bricks proved to be superior in hot condition as a result of numerous tests conducted within the company on alkaline resistance, hot-bending, and the hot volume stability of bricks. A comprehensive judgement based on these results led to the use of SiC-C bricks in the belly and lower shaft of No. 2 blast furnace for the third campaign.

5.2 Thermal Expansion Margin in Brick Work in the Furnace Body

In the conventional brickwork for blast furnace, a few places are left as margin for thermal expansion in the belly and shaft, and this is believed to cause the bricks to fall in the early stages after blowing-in.

This time, the necessity of such thermal expansion margin was studied in light of analysis of elasticity stress employing the finite element method. **Fig. 12** shows the temperature distribution of bricks which was the basic condition for the above analysis, and **Figs. 13** and **14** show the results of the analysis. In **Fig. 13**, where 3 expansion margins have been provided, most of the thermal expansion in the bricks is alleviated by contraction of the joints, with little absorption by the thermal expansion margins. **Fig. 14** shows that with or without thermal expansion margins, the stress in bricks and shell plates hardly changes.

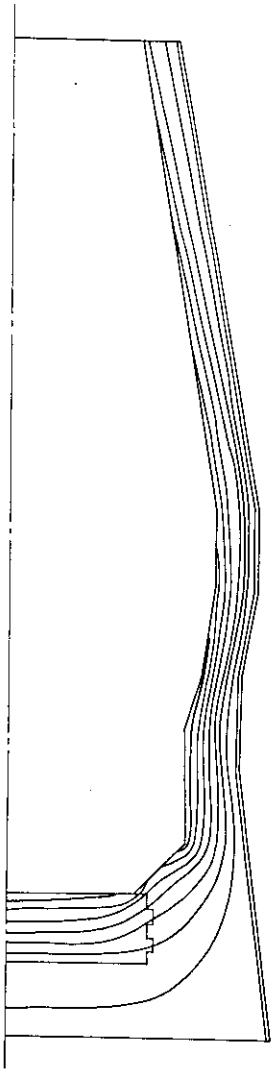

Fig. 12 Temperature distribution in blast furnace wall and bottom presumed for calculation

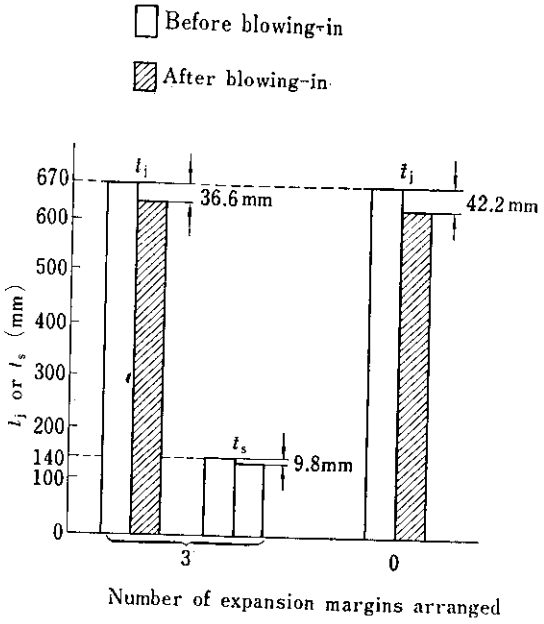

Fig. 13 Calculated changes of total joint thickness, t_j, and total expansion margin, t_s, in the brick work-during the early stage of blast furnace operation after blowing-in

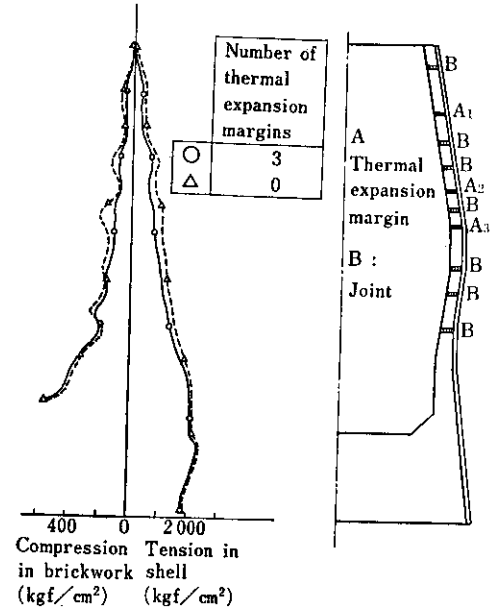

Fig. 14 Calculated vertical distribution of stress in BF shell and brickwork

Therefore, it was decided that there was little need to create thermal expansion margins. In this reconstruction, thermal expansion margins were not created; instead, bricks were arranged so that thermal expansion would be absorbed by the joints.

Changes in axial stress measured in No. 2 blast furnace shell in the third campaign are indicated in **Fig. 15**. Figures in **Fig. 15** are smaller than those in **Fig. 14**, which proves that the removal of thermal expansion margins does not create any problems.

5.3 Estimation of Brick Erosion in the Furnace Bottom

An accurate estimate of erosion conditions in the furnace bottom which is its critical part can lead to measures to prolong the furnace life through proper actions taken in the phases of equipment and operation. Keeping this objective in mind, various calculations were performed to estimate brick erosion at the furnace bottom, mainly using No. 2 blast furnace after the second campaign, with its bottom temperature unusually high. An example of isotherms in the furnace

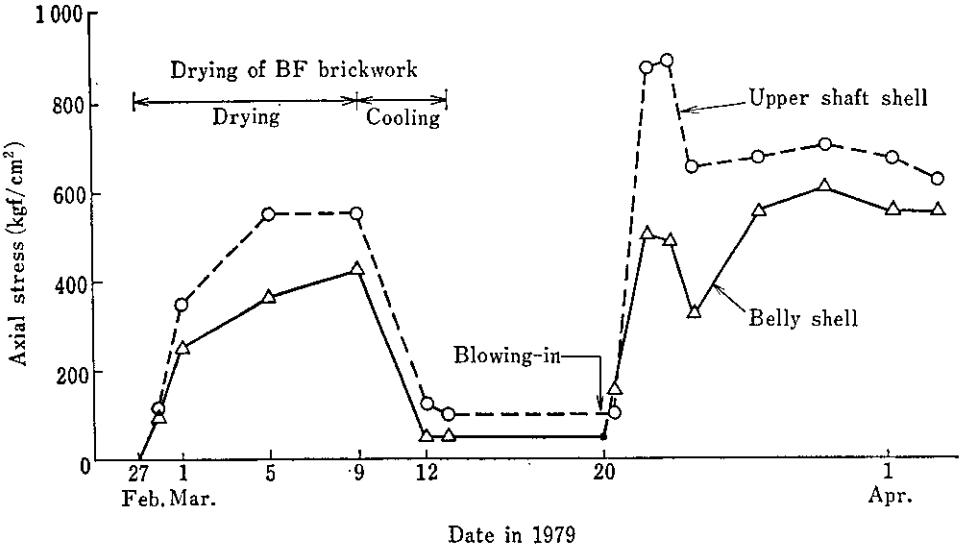

Fig. 15 Change of axial stress measured in No. 2 BF shell

bottom calculated using the finite element method is shown in **Fig. 16.**

These calculated brick erosion estimates were compared with results from analysis data obtained from the disjointing of the blast furnace in reconstruction for the third campaign. The following facts were found:

(1) When the erosion trend in the bottom brick of No. 2 blast furnace for the second campaign is calculated using the finite element method, a noticeable erosion advances in the early stage after blowing-in, gradually reaching its levelling off (see **Fig. 17**).

(2) According to heat transfer calculations after equilibrium is reached, the isotherm of 1 150°C is almost identical to the actual erosion line of the bricks.

In the reconstruction of No.2 blast furnace for the third campaign, the thermocouples were placed in the furnace bottom as indicated in **Fig. 18**. This figure is based on the above-mentioned research, and contributes to an accurate estimation of erosion in furnace bottoms, which is calculated through heat transfer analysis employing the finite element method. This figure can also be used to aid in the control of the furnace bottom during operation.

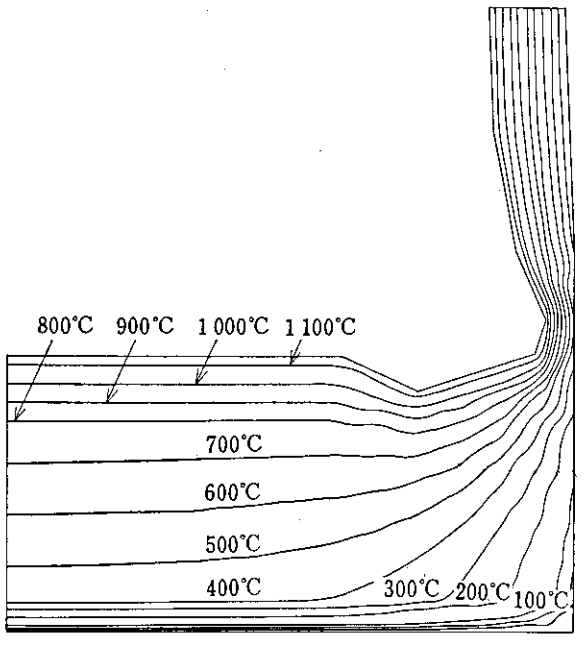

Fig. 16 Isotherms in blast furnace bottom calculated by finite element method

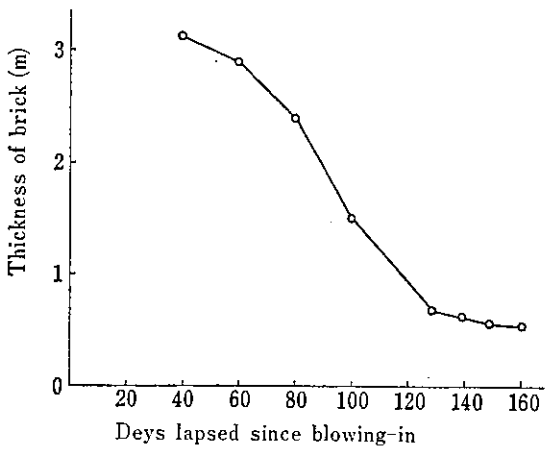

Fig. 17 Erosion trend of blast furnace bottom calculated by finite element method

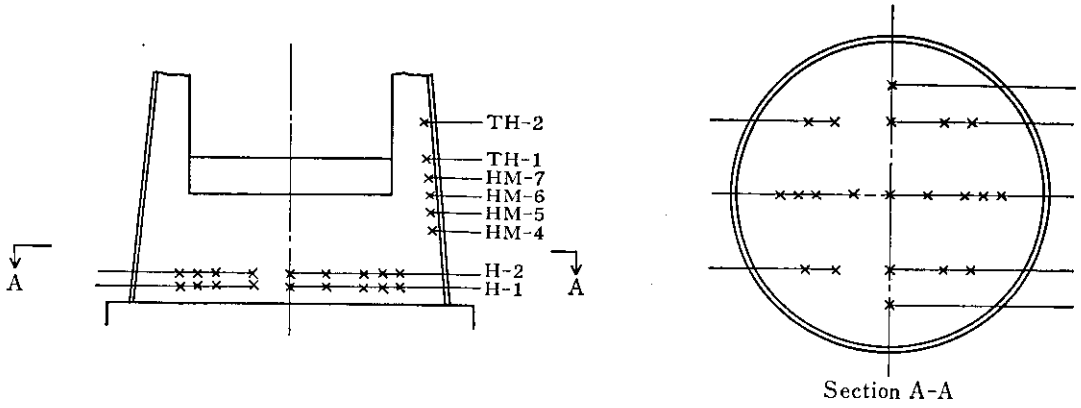

Fig. 18 Location of thermocouples in blast furnace bottom

6 Auxiliary Facilities

6.1 Dust Collector for the Cast House

The dust collector for the cast house was constructed with emphasis placed on energy conservation and development of an efficient fume collecting method.

6.1.1 Dust collecting hood

The dust collecting hood of retractable type was developed for secondary dust collection at cast house. Its details are shown in the previous technical report.

6.1.2 Control system

The wind volume of the retractable hood for secondary dust collection and of the local dust collections has a suction pattern set in accordance with the dust emission rate. Because pressure loss in ducts differs according to various dust collecting duct routes and suction conditions, the rotation speeds of fans and operation of the damper during suction are controlled by a micro computer to suit suction conditions. An automatic conditions dust collecting system was thus developed. With this system, a series of processes, including damper operation and dust collecting wind volume control, can be automatically controlled simply by pressing buttons.

Suction pattern and pressure loss in the duct (calculated values) are shown in **Figs. 19** and **20.**

The adoption of this system has greatly reduced energy consumption.

6.2 Slag Sand Manufacturing Plant

A project team which intended to establish production techniques for slag sand, developed a **K-N** (Kawatetsu-Nagata) type molten slag cooler. The first unit of this type was attached to No. 2 blast furnace for the third campaign during reconstruction. Details are given in a separate technical report[7].

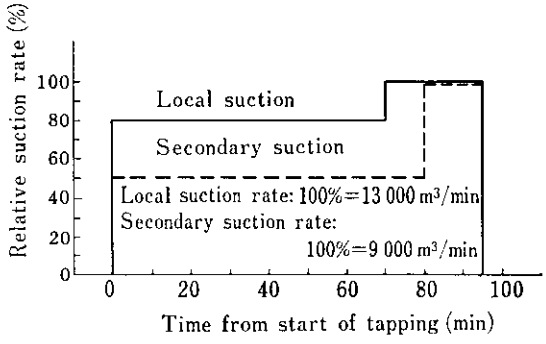

Fig. 19 Suction pattern for cast house emission control

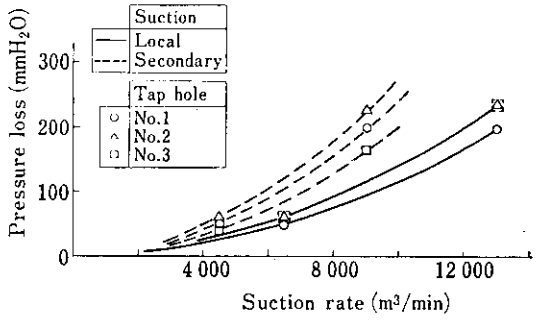

Fig. 20 Pressure loss in duct in relation with suction rate

7 Conclusion

This report is an outline centering on technological features in the reconstruction of the Mizushima No. 2 blast furnace for the third campaign.

No. 2 blast furnace has experienced very little equipment trouble, and it has operated well since its blowing-in. Reconstruction this time was more successful than at previous times when more conventional methods were used. Regarding its operation, the furnace achieved a world record-breaking fuel ratio of 426 kg/t-pig per month (average) in February 1980. Thus, the blast furnace is in very good condition in both operation and equipment, giving all concerned a confidence in the company's own reconstruction methods.

References

1) I. Yamashita, et al.: *Kawasaki Steel Technical Report*, **12** (1980) 2, pp. 148–158 (in Japanese)
2) V. Paschkis, Taghi Mirsepassi: *Iron and Steel Engineer*, (1956) 6, p. 116
3) Robert D. Pehlke, Gary S. Hening: *Canadian Metallurgical Quarterly*, **15** (1976) 1, p. 83
4) T. Hiratani, T. Nishiyama, I. Ichihara: *Tetsu-to-Hagané*, **60** (1974) 10, A79
5) M. Saitoh, H. Shintani, I. Ohishi: *Tetsu-to-Hagané*, **65** (1979) 11, S539
6) T. Ishihara, et al.: *Kawasaki Steel Technical Report*, **12** (1980) 2, pp. 174–177 (in Japanese)
7) H. Tanaka, et al.: *Kawasaki Steel Technical Report*, **12** (1980) 2, pp. 56–64 (in Japanese)